

Exciting Novel Polyaspartates: Design, Synthesis, and Photo-Responsive Behavior in Solution and Lyotropic Liquid Crystalline Phase Upon Irradiation with Visible Light

Rimjhim Hossain and Christina M. Thiele*

Many polypeptides form stable, helical secondary structures enabling the formation of lyotropic liquid crystalline (LLC) phases. Contrary to the well-studied polyglutamate, their counterparts based on polyaspartates exhibit a much lower helix inversion barrier. Therefore, the helix sense is not solely dictated by the chirality of the amino acid used, but additionally by the nature and conformation of the polymer sidechain. In this work, polymers responsive to irradiation with visible light are designed achieving conformational transitions from helix-to-coil and helix-to-helix. The synthesis and the application as LLC mesogens of several (co-)polyaspartates bearing *ortho*-fluorinated azobenzene (FAB) as a photochromic group are presented. Many of the obtained polymers undergo changes in their secondary structure upon *E-Z*-isomerization of the FAB-containing sidechain. Of special interest are copolymers that exhibit photo-responsive helix inversion without loss of their helical secondary structure. These copolymers form stable LLC phases in helicogenic solvents, where the effect of photo-switching on the macroscopic behavior is studied by NMR spectroscopy. Especially, the irradiation of the different LLC phases of the helix inversion polymers displays a change in the LLC order experienced by the solvent. These peculiar properties are promising for future applications as photo-responsive alignment media for structure elucidation in NMR.

like optoelectronics,^[3,4] bio- and chemosensing,^[5] catalysis,^[6] biomedical nanomaterials,^[7,8] membranes,^[9,10] etc. The responsiveness can be achieved by applying various external stimuli such as temperature, mechanical force, magnetic and electric fields, voltage, additives, changes in pH and light. Among these stimuli, light is particularly advantageous due to the easy applicability (ex situ or in situ), controlled localized and temporal use, the precise tunability of light (wavelength, linear- or circular-polarized, intensity, etc.), and the non-invasive nature.^[11] A widespread strategy to achieve light responsiveness is the incorporation of molecular switches such as diarylethenes,^[12,13] spiropyranes,^[14] donor-acceptor Stenhouse adducts (DASAs),^[15] and azobenzenes,^[16,17] which undergo reversible structural and conformational changes. Especially, the reversible *E-Z*-isomerization of azobenzene derivatives resulting in changes in polarity, geometry, and dipole moment is exploited widely in material science.^[16–18] Among the smart materials known, polymers stand out as the choice of polymer architecture (topology,

composition, functionality, secondary structure, etc.) allows tailoring of the resulting properties to a specific application.^[19,20] When considering chiral polymers, the helix is a well-known and sought-after structural motive, among which polypeptides, especially polyaspartates and polyglutamate have received attention. The chiral polypeptide backbone can form helical conformations in solution, creating rod-like segments.^[21] For polyglutamates, the resulting helix sense is solely dictated by the chirality of the monomer(s) used with high energy barriers for the inversion of this helix sense. Therefore, poly(L-glutamates) always form right-handed helices, whereas poly(D-glutamates) form left-handed helices. Contrary to that, poly(L-aspartates) exhibit a unique feature by forming α -helical structures with opposing helix sense depending on the nature of the moiety in the sidechain^[22] resulting from a reduction of the energy barrier for helix inversion.^[23] Sidechain variations such as -methyl, ethyl-, propyl, nitrobenzyl-, *p*-chlorobenzyl groups, and several others have substantiated the dynamic character of polyaspartates (Figure 1).^[23–27]

Benzylic residues (benzyl-L-aspartate, BLA) adopt stable left-handed helices resulting from the favored interaction of the

1. Introduction

Smart materials are an emerging field in recent research due to the alteration in their physical and chemical properties as response to environmental changes.^[1,2] This (multi-)functional nature of smart materials is exploited in many fields

R. Hossain, C. M. Thiele
 Clemens-Schöpf-Institute for Organic Chemistry and Biochemistry
 Technical University of Darmstadt
 Peter-Grünberg-Straße 16, 64287 Darmstadt, Germany
 E-mail: cthiele@thielelab.de

 The ORCID identification number(s) for the author(s) of this article can be found under <https://doi.org/10.1002/marc.202400513>

© 2024 The Author(s). Macromolecular Rapid Communications published by Wiley-VCH GmbH. This is an open access article under the terms of the [Creative Commons Attribution-NonCommercial-NoDerivs](https://creativecommons.org/licenses/by-nc-nd/4.0/) License, which permits use and distribution in any medium, provided the original work is properly cited, the use is non-commercial and no modifications or adaptations are made.

DOI: 10.1002/marc.202400513

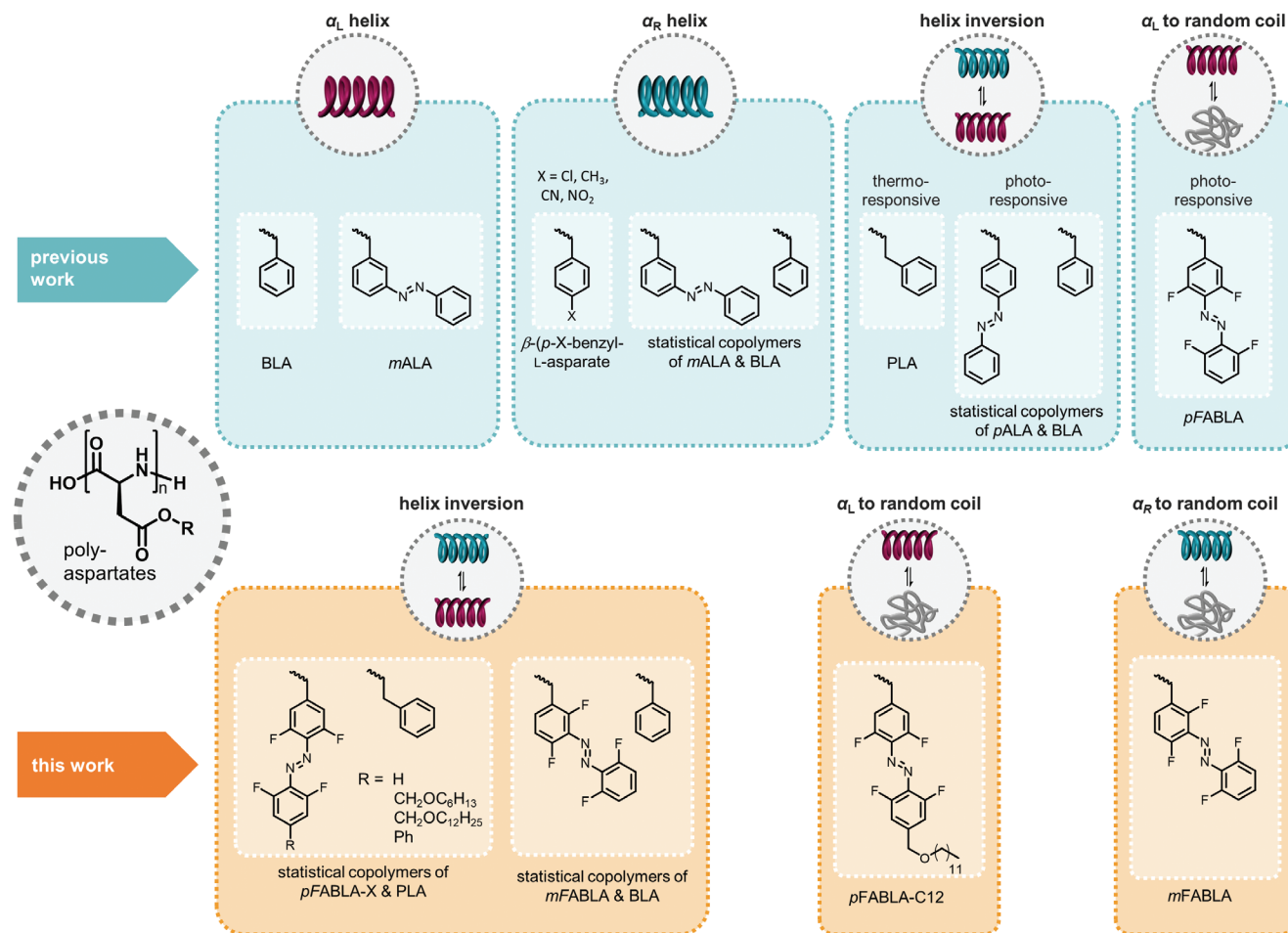


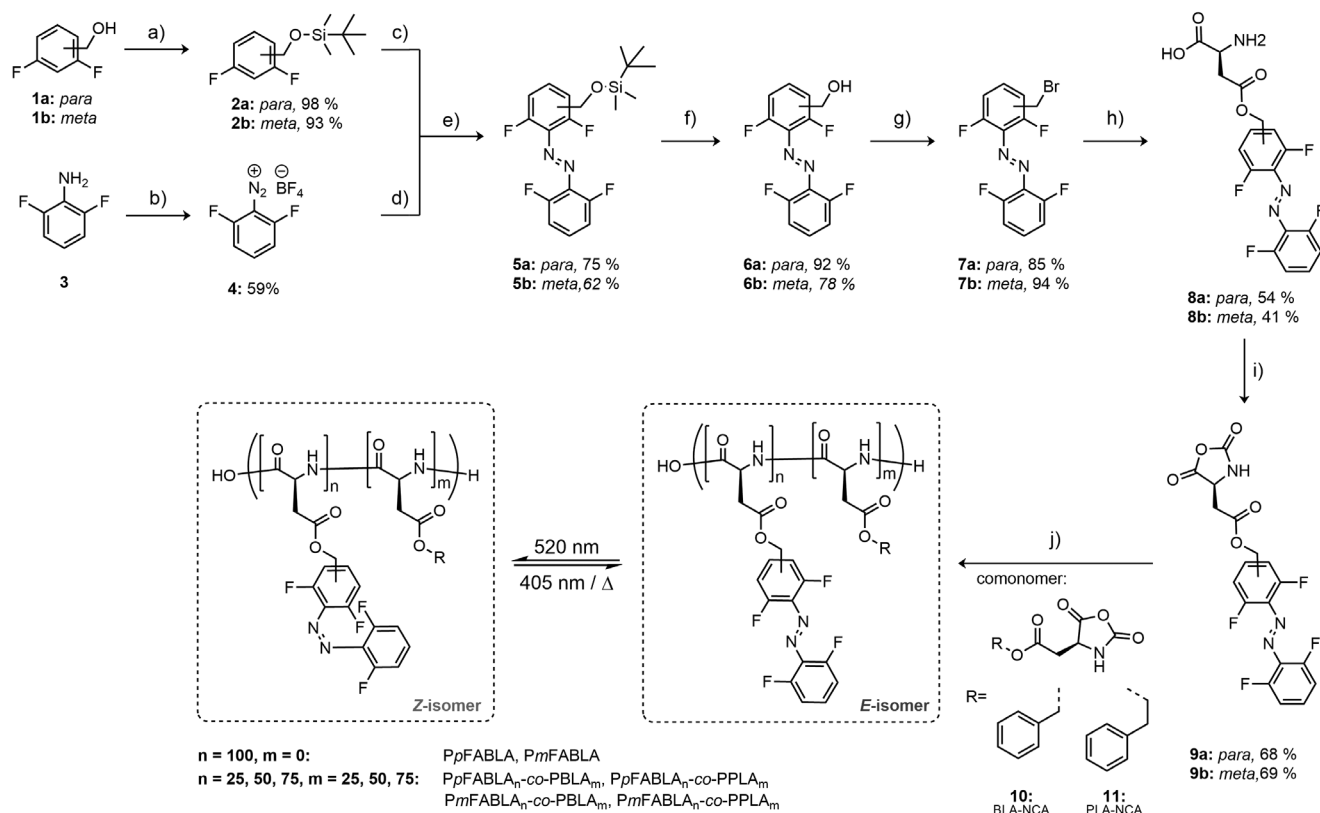
Figure 1. Influence of sidechain structure of (co-)polyaspartates on the secondary structure (α_L , α_R) and the stimuli-responsive conformational transitions (helix-to-helix, helix-to-coil) in chlorinated solvents shown in previous work^[23–27] and this work.

γ -carbonyl group with amide groups in the main chain.^[28,29] Introduction of an additional CH_2 group as in the phenethyl-L-aspartate (PLA) leads to α_R -helical screw-sense at low temperature. For PLLA, a helix sense inversion to left-handed helices takes place when increasing the temperature. This thermo-responsiveness was studied in dilute solution and liquid crystalline state to elucidate the helix inversion mechanism and sidechain conformational behavior by ABE et al.^[30,31] The response temperature could be modulated for statistical copolymers comprised of benzyl- and phenethyl-L-aspartates (PBLA-co-PPLA) by variation of the monomer composition.^[32,33] Thus, polyaspartates seem well-suited to investigate whether photochromic groups have an impact on their secondary structure.^[34]

For a series of statistical copolyaspartates with β -benzylic- and β -(*para*-phenylazobenzyl)-L-aspartate pALA (PpALA-co-PBLA) in the sidechain, helix inversion of the polymer occurred as a function of azobenzene content. For polymers with less than 50 % of azobenzenes in the sidechain, the α_L helical structure was preserved in 1,2-dichloroethane (DCE) as solvent irrespective of the photo-isomers of the azobenzene being present. For high azobenzene contents, however, photo-induced helix-to-helix transitions in DCE are observed.^[35] In addition, the conformational transi-

tions are modulated by varying the composition of the solvent mixtures such as DCE/hexafluoroisopropanol (HFIP), whereas a helix-to-helix transition only occurs for high contents of HFIP (35 %).^[36] The choice of solvent or solvent mixture thus has a major impact on the polymer's photo-responsive behavior in solution.^[36,37] Ueno et al. also investigated the influence of β -(*meta*-phenylazo)-benzylic (*m*ALA) groups in the sidechain and found a different conformational behavior for the corresponding copolyaspartates in DCE. Interestingly, the minor change in substitution pattern causes the disappearance of helix inversion irrespective of the azobenzene content. Solely, a decrease in helicity could be determined via circular dichroism spectroscopy.^[35,38]

Recently our group has conducted studies by incorporating *ortho*-fluorinated azobenzenes (FAB) as molecular switches, for which *E-Z*-isomerization can be induced with visible light. Compared to the non-fluorinated azobenzenes, the separation of the $n \rightarrow \pi^*$ absorption bands of the two photo-isomers is increased, enabling selective photo-isomerization with high contents of *E*- and *Z*-isomers in each photo-stationary state (PSS). Both isomers are reported to be stable at ambient temperature (bi-stability) enabling long-term investigations of each state (interim/photo-stationary).^[39,40] Hirschmann et al. presented a homopolymer with *para*-substituted FAB moieties in the sidechain exhibiting



Scheme 1. Nine-step synthetic procedure with experimental details yielding (co-)polyaspartates (PpFABLA_n-co-PBLA_m, PpFABLA_n-co-PPLA_m, PmFABLA_n-co-PBLA_m, PmFABLA_n-co-PPLA_m, with n = 25, 50, 75, m = 25, 50, 75) derived from *p*FABLA-NCA **9a**, *m*FABLA-NCA **9b**, BLA-NCA **10**, and PLA-NCA **11**. a) TBDMS-Cl, imidazole, in DCM dry, 0 °C to rt, 16 h; b) 1. HBF₄ (50% aq.), 2. NaNO₂ in water, 0 °C, 2 h; c) *n*-BuLi in THF abs., -78 to -20 °C, 1 h; d) in THF abs., -78 °C, e) -78 °C to rt; f) TBAF in THF abs., 0 °C to rt, 2 h, overnight, g) PPh₃, NBS in THF abs., 0 °C to rt, 2 h; h) 1. Cu(L-Asp)₂·8 H₂O, *N,N,N',N'*-tetramethylguanidine (TMG), in DMF/water, rt, 1 h, 2. 60 °C, overnight; i) phosgene (2.5 M in toluene), α -pinene in THF abs., 50 °C, overnight; j) DMEA in DCM abs./THF abs.

a helix-to-coil transition in dilute solution under irradiation with visible light. This behavior was also observed to induce macroscopic order-to-disorder transformation in the liquid crystalline state. The lyotropic liquid crystalline (LLC) phases were applied as photo-responsive alignment media giving access to isotropic and anisotropic NMR observables from the same sample, which opened up new avenues in structure elucidation in NMR spectroscopy based on residual dipolar couplings (RDC).^[41–43] To enhance the structural information for a complex analyte, the determination of multiple sets of RDCs is necessary, requiring different alignment media or switchable alignment media with various orientations in the liquid crystalline state.^[43–46] For this purpose, we aim for photo-induced order-to-order transitions in the lyotropic liquid crystalline state based on polyaspartates with various FAB derivatives as switchable helical scaffolds. Herein, *para*-substituted and *meta*-substituted FAB are incorporated into polyaspartates to investigate the influence of geometrical changes in the sidechain. Additionally, alkyl groups such as hexyl- and dodecyl-substituents improving solubility in common organic solvents are introduced in *para*-positions to the azo group. In addition to the synthesis of homopolymers with varying FAB-moieties, we show that light-induced conformational transitions can be accessed by copolymerization of FAB-monomers with non-photo-switchable comonomers with opposing helical sense

(BLA, PLA) to lower the energy barrier for helix inversion. The influence of the different comonomer ratios on the conformational transitions in the resulting polymers is investigated in dilute solutions by CD spectroscopy and lyotropic liquid crystalline state via ²H NMR spectroscopy.

2. Results and Discussion

2.1. Syntheses

Novel photo-responsive (co-)polyaspartates with *para*- and *meta*-substituted FAB derivatives in the sidechain were synthesized via a nine-step procedure (**Scheme 1**). For (co-)polyaspartates with substituents attached to the FAB-moieties (*p*FABLA-C6, *p*FABLA-C12, *p*FABLA-Ph) in the sidechain, additional steps were necessary to synthesize the modified starting material (for more detail see **SI**, Supporting Information). Esterification with *L*-aspartic acid to yield esters **8a–e** and formation of *N*-carboxyanhydrides (NCAs) **9a–e** represent essential steps in the procedure.^[47] Finally, ring-opening polymerization of NCAs leads to the corresponding polypeptides.^[48,49]

Following literature-known procedures,^[50,51] silyl ethers **2a–b** were synthesized from the corresponding benzylic alcohols **1a–b**. Diazonium salt **4** was obtained from amine **3**. Compounds **2a–b**,

Table 1. (Co-)polyaspartates with experimental comonomer ratio $[M_1]/[M_2]_{\text{exp}}$, number averaged molecular weight $M_{n,\bar{1}}$, polydispersity \bar{D} . Targeted comonomer ratios are given as an index in the polymer designation.

Entry	Polymer	$[M_1]/[M_2]_{\text{exp}}$	$M_{n,\bar{1}}/[\text{kg}^*\text{mol}^{-1}]^{\text{a}}$	\bar{D}	Batch (RH03-#)
1	PpFABLA	–	65.2	1.60	301
2	PpFABLA _{75-co-PBLA} ₂₅	79/21	87.6	1.41	204
3	PpFABLA _{50-co-PBLA} ₅₀	52/48	126.0	1.37	201
4	PpFABLA _{25-co-PBLA} ₇₅	27/73	145.0	1.20	206
5	PpFABLA _{75-co-PPLA} ₂₅	80/20	107.9	1.32	205
6	PpFABLA _{50-co-PPLA} _{50^b}	51/49	121.0	1.39	202
7	PpFABLA _{50-co-PPLA} ₅₀	52/48	129.0	1.81	300
8	PpFABLA _{25-co-PPLA} ₇₅	24/76	129.9	1.26	207
9	PmFABLA	–	14.6	1.28	257B
10	PmFABLA _{75-co-PBLA} _{25^b}	75/25	40.6	1.37	261
11	PmFABLA _{50-co-PBLA} ₅₀	50/50	48.2	1.66	262
12	PmFABLA _{25-co-PBLA} ₇₅	30/70	85.7	1.26	263
13	PmFABLA _{75-co-PPLA} ₂₅	75/25	50.2	1.22	258
14	PmFABLA _{50-co-PPLA} ₅₀	52/48	77.1	1.11	259
15	PmFABLA _{25-co-PPLA} ₇₅	26/74	150.1	1.28	260
16	PpFABLA-C6	–	100.8	1.99	275
17	PpFABLA-C6 ^b	–	18.6	1.46	NS02-14
18	PpFABLA-C6 _{50-co-PPLA} ₅₀	53/47	38.4	1.33	293
19	PpFABLA-C12 ^b	–	35.9	1.26	NS02-13
20	PpFABLA-C12	–	14.4	1.20	295
21	PpFABLA-C12 _{50-co-PPLA} ₅₀	53/47	26.2	1.43	294
22	PpFABLA-Ph _{50-co-PPLA} ₅₀	47/53	60.2	9.93	292

^a) SEC samples were irradiated at 405 nm for 10 min each (PSS-E); ^b) Irradiation at 520 nm for 10 min (PSS-Z) was applied to exemplarily show that no significant dependency of the molecular weight distribution on the isomerization state was observed (for more detail, see SI).

and **4** are applied as building blocks in the following azo-coupling reaction. Lithiation of ethers **2a-b** with *n*-butyllithium under inert conditions and subsequent coupling with diazonium salt **4** produced *para*- and *meta*-substituted FAB-silyl ethers **5a-b**.^[51] The *p*- and *m*-FAB-benzylic alcohols **6a-b** were obtained via a deprotection procedure using *tert*-butylammoniumfluoride (TBAF) according to the literature.^[50] Subsequent bromination was carried out under mild conditions using *N*-bromosuccinimide (NBS) and PPh₃ as reagents producing benzylic bromides **7a-b** in high yields.^[52] Selective esterification was performed with a copper-aspartic-acid complex to give respective FAB-modified aspartates **8a-b** following a modified procedure.^[47] For the synthesis of the NCAs **9a-e**, α -pinene and an excess of phosgene was applied.^[53] As the purity of the synthesized NCA is crucial for the success of polymerization, moisture-free column chromatography was implemented as the purification method. Comonomers **10** and **11** were synthesized and purified via two steps following the literature procedures.^[54–56] Finally, the ring-opening (co-)polymerization was carried out with *N,N*-dimethylethanolamine (DMEA) as the initiator.^[57,58] The successfully synthesized (co-)polyaspartates with their averaged molecular weights and dispersities are given in **Table 1**. For copolymers, the targeted monomer ratios are given as an index in

the respective polymer designation. Experimentally achieved monomer ratios $[M_1]/[M_2]_{\text{exp}}$ in copolymers, where M_1 refers to the FAB-NCAs (*p*FABLA-NCA, *m*FABLA-NCA, *p*FABLA-C6-NCA, *p*FABLA-C12-NCA, *p*FABLA-Ph-NCA) and M_2 to the non-photo-switchable NCA (BLA-NCA, PLA-NCA) as the monomer, were determined via ¹H spectra (for more details see SI).

Progress of polymerization was monitored by IR spectroscopy^[59] and complete conversion was reached after 6–23 days, dependent on the relative amount of FAB-monomer in solution. The increased polymerization time observed for FAB monomers could arise due to their larger steric demand or due to the competing interactions of initiators/active chain ends with nitrogen-containing FAB moieties. Residual impurities, invisible to the analytical methods employed, would lead to a termination of active chain ends in polymerization. As the molecular weight distributions are narrow and monomodal, it is assumed that the termination of active chain ends is negligible. In two cases, namely homopolymer PmFABLA (**Table 1**, entry 9) and copolymer PpFABLA-Ph_{50-co-PPLA}₅₀ (**Table 1**, entry 22), polymerizations were terminated at incomplete conversion after ≈ 80 days. No PpFABLA-Ph homopolymer could be obtained, presumably due to the causes previously mentioned. Next, the influence of the sidechain photo-isomerization on the secondary structure of the obtained polymers is studied via CD spectroscopy.

2.2. Photo-Switching Behavior in Dilute Solution

To analyze the conformational transitions of the obtained (co-)polyaspartates qualitatively, CD- and simultaneously acquired UV/Vis-spectra of dilute solutions in helicogenic organic solvents such as 1,1,2,2-tetrachlorethane (TCE)^[60] and dichloromethane (DCM)^[61] were measured after irradiation at 405 nm (*Z*→*E*, PSS-*E*) and 520 nm (*E*→*Z*, PSS-*Z*). Characteristic CD bands at ≈ 225 nm (amide band) were assigned to an α -helical structure of polyaspartates according to the literature.^[62] The sign of the $n \rightarrow \pi^*$ transition at 225 nm correlates to the helix sense, where a positive sign is interpreted as α_L -helix and a negative sign as α_R -helix, respectively. These are summarized for the obtained polymers in PSS-*E* and PSS-*Z* in **Table 2** (full CD spectra are given in SI). The concomitant measurement of UV-vis spectra confirms that a photo-stationary state is reached after irradiation. The obtained polymers show absorption bands equivalent to the FAB-derivatives (full UV-vis spectra are given in SI). In the following, the findings from CD spectra in TCE as solvent (**Table 2**, entry 1–22) are discussed first.

The influence of different FAB motifs in the polymer sidechain was determined by comparing the CD spectra of the synthesized homopolymers in PSS-*E* and PSS-*Z*. After irradiation at 405 nm, producing PSS-*E*, a dilute solution of PpFABLA homopolymer in TCE exhibits a positive CD signal at 225 nm (**Table 2**, entry 1). Irradiation of the identical sample with 520 nm leads to isomerization to PSS-*Z* resulting in a significant decrease of the CD band. Photo-isomerization from *E*→*Z* of FAB in the sidechain thus results in an overall decrease of helical content of the polymer backbone.^[72] A similar photo-switching behavior is observed for the homopolymers PpFABLA-C6 (**Table 2**, entries 16,17) and PpFABLA-C12 (**Table 2**, entries 19,20) in TCE with a positive

Table 2. (Co-)polyaspartates with their helix sense α_x determined from the CD signal at 225 nm, with $x = L, R,$ or $0,$ (for cases where the CD signal is zero at that wavelength, details see text), and “red” indicating reduced intensity of the CD signal. CD spectra of dilute polymer solutions (0.5 wt.% in TCE using customized demountable cuvettes^[63] with a path-length < 0.01 mm; 0.05 wt.% in DCM using commercially available 1 mm cuvettes) were acquired after irradiation at 405 nm ($Z \rightarrow E,$ PSS- E) and 520 nm ($E \rightarrow Z,$ PSS- Z) for 10 min each. Polymers with photo-responsive helix-to-helix transition (helix inversion) are highlighted in orange.

Entry	Polymer	Solvent	α_x in PSS- Z	α_x in PSS- E	BatchRH03-##
1	PpFABLA	TCE	L (red.)	L	301
2	PpFABLA ₇₅ -co-PBLA ₂₅	TCE	L	L	204
3	PpFABLA ₅₀ -co-PBLA ₅₀	TCE	L	L	201
4	PpFABLA ₂₅ -co-PBLA ₇₅	TCE	L	L	206
5	PpFABLA ₇₅ -co-PPLA ₂₅	TCE	L (red.)	L	205
6	PpFABLA ₅₀ -co-PPLA ₅₀	TCE	R	L	202
7	PpFABLA ₅₀ -co-PPLA ₅₀	TCE	R	L	300
8	PpFABLA ₂₅ -co-PPLA ₇₅	TCE	R	R (red.)	207
9	PmFABLA	TCE	0	R	257B
10	PmFABLA ₇₅ -co-PBLA ₂₅	TCE	R	L	261
11	PmFABLA ₅₀ -co-PBLA ₅₀	TCE	0	L	262
12	PmFABLA ₂₅ -co-PBLA ₇₅	TCE	L (red.)	L	263
13	PmFABLA ₇₅ -co-PPLA ₂₅	TCE	R	R	258
14	PmFABLA ₅₀ -co-PPLA ₅₀	TCE	R	R	259
15	PmFABLA ₂₅ -co-PPLA ₇₅	TCE	R	R	260
16	PpFABLA-C6	TCE	L (red.)	L	275
17	PpFABLA-C6	TCE	L (red.)	L	NS02-14
18	PpFABLA-C6 ₅₀ -co-PPLA ₅₀	TCE	R	L	293
19	PpFABLA-C12	TCE	0	L	NS02-13
20	PpFABLA-C12	TCE	L (red.)	L	295
21	PpFABLA-C12 ₅₀ -co-PPLA ₅₀	TCE	R	L	294
22	PpFABLA-Ph ₅₀ -co-PPLA ₅₀	TCE	R	L	292
23	PpFABLA	DCM	L	L	301
24	PpFABLA ₅₀ -co-PPLA ₅₀	DCM	L	L	300
25	PpFABLA-C6	DCM	L	L	NS02-14
26	PpFABLA-C6 ₅₀ -co-PPLA ₅₀	DCM	L	L	293
27	PpFABLA-C12	DCM	L	L (red.)	NS02-13
28	PpFABLA-C12 ₅₀ -co-PPLA ₅₀	DCM	L (red)	L	294

CD signal at 225 nm in PSS- E indicating a α_L helical structure. In PSS- Z , the amide bands decrease significantly, for the higher molecular weight PpFABLA-C12 sample (entry 20) even until complete depletion implying a disordered structure (random coil). A potential explanation could be the smaller distance between the bulky alkyl groups to the helical backbone in PSS- Z as in PSS- E . This steric effect presumably leads to a (partial or total) collapse of the helical structure. However, in PSS- E , the alkyl groups are presumed to be further away from the helix, therefore the formation of the helical structure is less hindered. In contrast to the *para*-substituted homopolymers, the homopolymer with the *meta*-substitution pattern PmFABLA exhibits a strongly negative amide band in PSS- Z (α_R helical structure) and CD = 0 in PSS- E (Table 2, entry 9). Therefore, photo-induced interconversion of *meta*-substituted FAB in the sidechain results in a re-

versible transition from random coil to helix. Interestingly, additional CD bands above 250 nm are observed for all homopolymers (see full CD spectra in SI). These indicate either a chiral induction of handedness from the backbone to the azobenzene side chain^[65] or electronic interactions between the photochromes themselves.^[66,67]

To further study the influence of photo-induced sidechain interconversion on the helical backbone, copolymers with FAB- and non-photo-switchable monomers were synthesized varying the amounts of azobenzene. For this purpose, literature-known benzyl-substituted (BLA) and phenethyl-substituted (PLA) moieties are introduced. It is reported that BLA-derived homopolymers exhibit a left-handed helical structure, whereas PLA-derived homopoly-aspartates adopt right-handed helices at ambient temperature.^[24,27,29,68] No significant change in secondary structure is observed for PpFABLA-co-PBLA irrespective of the azobenzene content upon E - Z -isomerization in the sidechain (Table 2, entries 2–4). These findings are in line with expectations one can deduce from the respective homopolymers: PpFABLA in PSS- E and PBLA both adopt a left-handed helix so that a left-handed helix is favored for the copolymers. Thus, photo-isomerization to PSS- Z leads to a partial loss of helicity for PpFABLA, whereas the stable helical structure of PBLA remains unaffected resulting overall in the α_L helix configuration.

For copolymers comprised of pFABLA- and PLA-residues in the sidechain favoring opposing helical senses, it becomes apparent that a variation of the azo content leads to different helix sense of the main chain already in PSS- E (Figure 2, top): The incorporation of higher amounts of pFABLA units (PpFABLA₇₅-co-PPLA₂₅, Table 2, entry 5) results in left-handed helicity for the polymer in both photo-stationary states as the minor component PLA is overruled. In the case of equal quantities of pFABLA and PLA moieties (PpFABLA₅₀-co-PPLA₅₀, Table 2, entries 6,7), α_L helices are observed in PSS- E . After irradiation at 520 nm, the left-handed helical content (originally favored by pFABLA) decreases, allowing the helix inversion to α_R favored by PLA units. When an excess of PLA relative to pFABLA is present (PpFABLA₂₅-co-PPLA₇₅, Table 2, entry 8), a right-handed secondary structure is dictated by PPLA independent of photo-isomerization of the azobenzene in the sidechain.

As mFABLA units dictate α_R helices in PSS- E , its combination with BLA is the most promising for tailoring a helix-to-helix transition within this series. CD spectra of PmFABLA₇₅-co-PBLA₂₅ (Table 2, entry 10 and Figure 2, bottom) exhibit a negative signal in PSS- Z indicating a right-handed helical structure. Photo-isomerization until PSS- E is reached, yields a weaker positive CD signal, therefore indicating the α_L configuration. The observed helix inversion is interpreted to be a collapse of α_R -helical structure from mFABLA units and being overruled by the α_L helicity from BLA sidechains. Since the magnitude of CD-signal in PSS- E is lower, it is assumed that both, random coil and α_L helices, are partially present. Reduction of the relative mFABLA content in the polymer (PmFABLA₅₀-co-PBLA₅₀, Table 2, entry 11) produces CD = 0 in PSS- Z , which is interpreted to be either a depletion of signal due to equal amounts of α_R - and α_L -helices being present or formation of a disordered random coil (see section on LLC phases for the resolution of this ambiguity). Decreasing the relative mFABLA content further (PmFABLA₂₅-co-PBLA₇₅, Table 2,

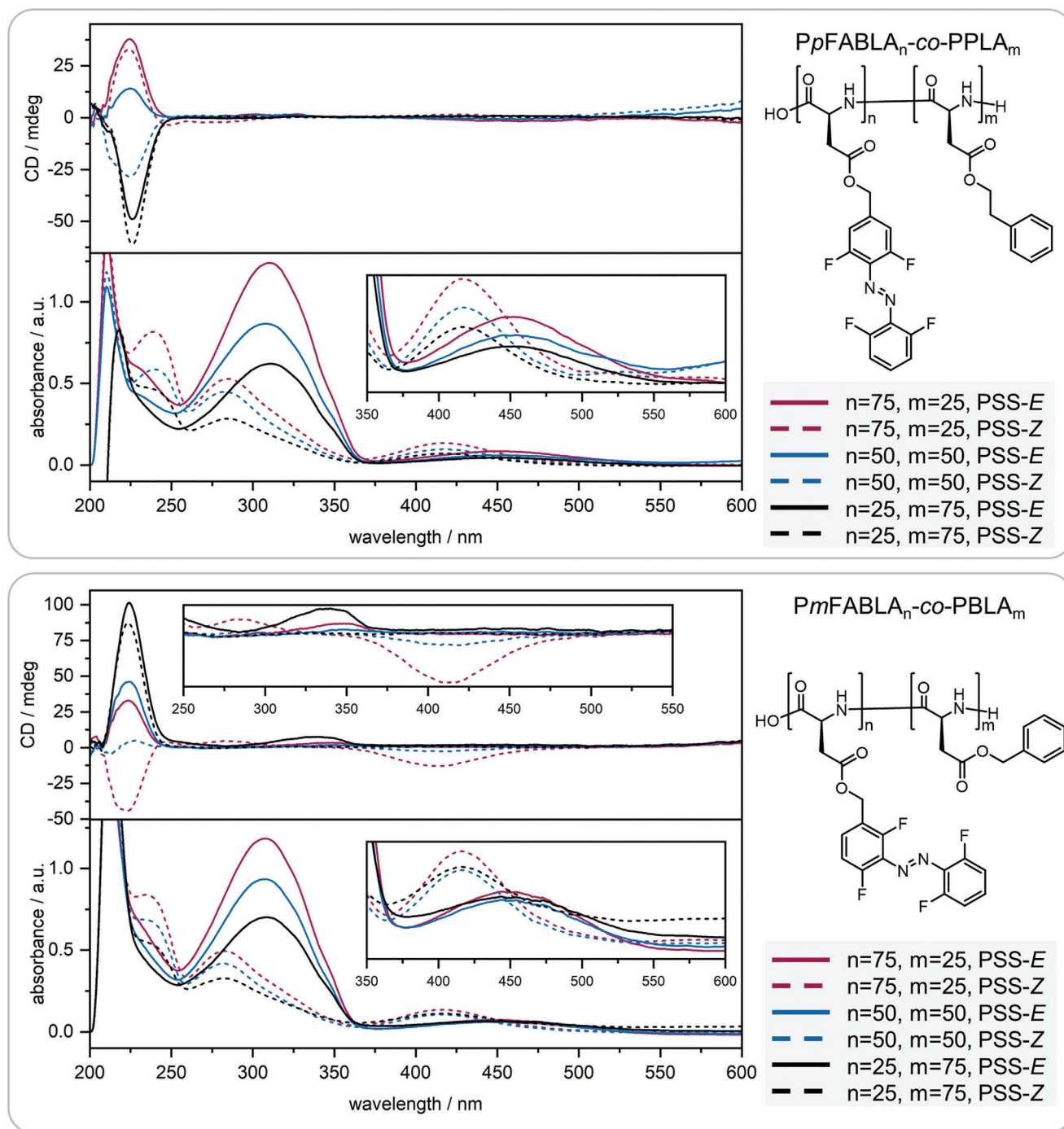


Figure 2. CD- and simultaneously acquired UV-vis-spectra of 0.5 wt.% solutions of copolyaspartates in TCE irradiated at 405 nm (PSS-E, solid lines) and 520 nm (PSS-Z, dashed lines) for 10 min each in demountable cuvettes^[63] with a pathlength of < 0.1 mm at 23 °C: PpFABLA_n-co-PPLA_m (top: RH03-205, -202, -207) and PmFABLA_n-co-PBLA_m (bottom: RH03-261, -262, -263).

entry 12) shows that photo-isomerization of the sidechain only has a minor effect on the intensity of the CD signal, but not the sign, with the helix thus remaining α_1 .

These findings show that photo-switchable conformational transitions such as helix inversion or the collapse of helical structure can be designed by combining two different moieties dictating opposing helical senses. Moreover, a transition occurs

only for high contents (above 50 %) of the photochromic unit. PmFABLA-co-PPLA (Table 2, entry 13–15) with different azobenzene contents (75 %, 50 %, and 25 %) show no switchability of the helix as expected from the fact that both moieties favor the same helix sense (see depicted CD spectra in SI).

Inspired by the success of the helix inversion polymer PpFABLA₅₀-co-PPLA₅₀, analogous polymers with alkyl groups

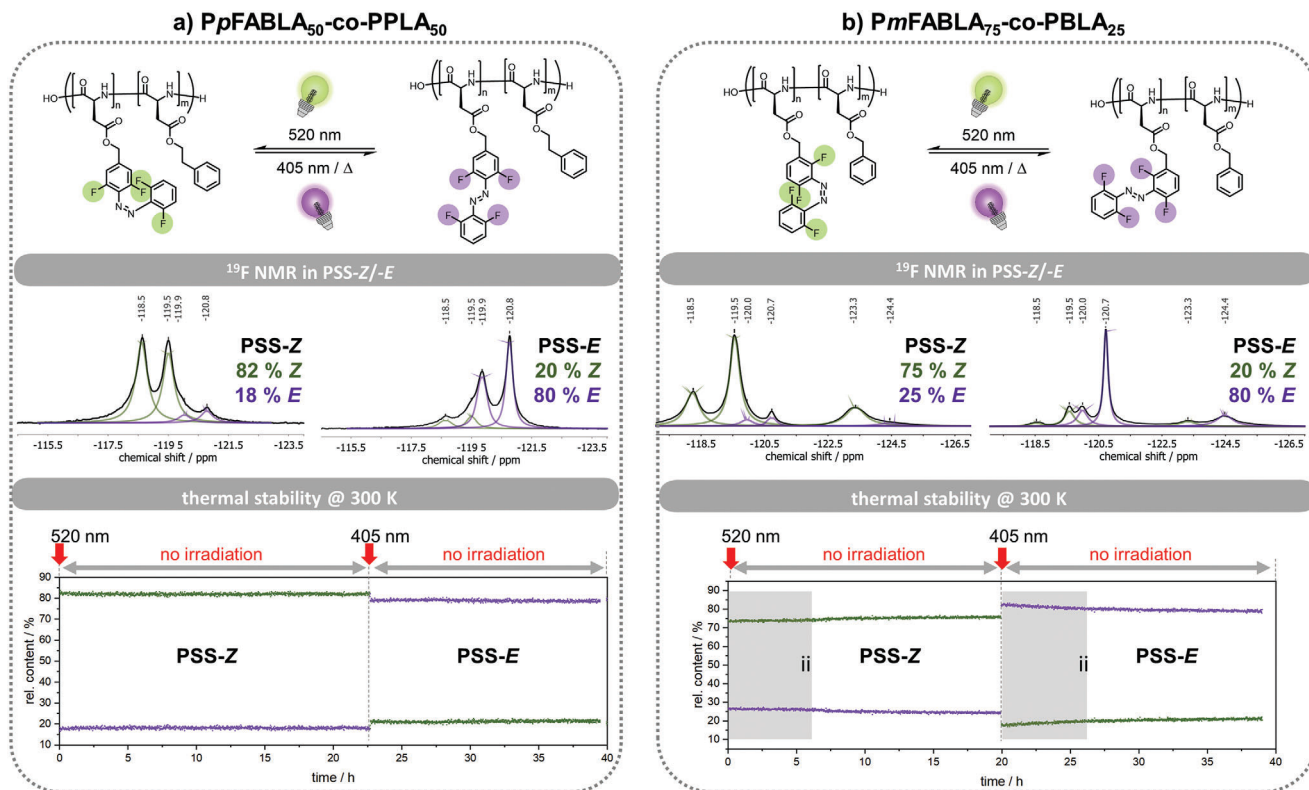


Figure 3. Thermal stability of isotropic polymer solutions in TCE- d_2 irradiated at 520 nm (PSS-Z) and 405 nm (PSS-E) at 300 K via series of ^{19}F NMR spectra (376 MHz): a) helix inversion polymer PpFABLA $_{50}$ -co-PPLA $_{50}$ (RH03-202), b) helix inversion polymer PmFABLA $_{75}$ -co-PBLA $_{25}$ (RH03-261).^[73]

PpFABLA-C6 $_{50}$ -co-PPLA $_{50}$ (Table 2, entry 18) and PpFABLA-C12 $_{50}$ -co-PPLA $_{50}$ (Table 2, entry 21) as well as PpFABLA-Ph $_{50}$ -co-PPLA $_{50}$ (Table 2, entry 22) were synthesized, and investigated for helix-to-helix transitions (see SI). A similar photo-induced helix inversion upon irradiation is observed in TCE as solvent for all three derivatives.

Subsequently, the influence of the solvent on the secondary structure is studied by measuring CD spectra in DCM as solvent (Table 2, entry 23–28). While these copolyaspartates undergo a helix inversion in TCE, they surprisingly form a stable left-handed helix in both PSS in DCM underlining the crucial effect of the solvent on the secondary structure. Also, the homopolymers PpFABLA, PpFABLA-C6, and PpFABLA-C12 exhibit an α_L structure irrespective of the photo-isomerization of the side chain.

After studying the secondary structure upon photo-isomerization via CD spectroscopy, the two polymers PpFABLA $_{50}$ -co-PPLA $_{50}$ and PmFABLA $_{75}$ -co-PBLA $_{25}$ showing helix inversion upon irradiation with visible light are examined concerning the thermal stability of the respective PSS at ambient temperature (bistability). Thus, *E*- and *Z*-isomers of the various synthesized pFAB and mFAB-derivatives can be quantitatively differentiated in ^{19}F NMR spectra as signals are baseline-separated (see SI). For the corresponding polymers slightly overlapping ^{19}F -signals are observed (see Figure 3, green: *Z*-isomer, violet: *E*-isomer). Characteristic areas for each isomer were integrated and deconvoluted to give the approxi-

mate composition in each photo-stationary state. High contents of *E*-isomer in PSS-*E* and *Z*-isomer in PSS-*Z* were obtained for both helix inversion polymers as shown in Figure 3.

After ex situ irradiation at 520 nm producing PSS-*Z*, series of ^{19}F -NMR-spectra were acquired at 300 K over several hours without further irradiation in the NMR spectrometer. The relative contents of *E*- and *Z*-isomers are plotted against time showing no significant change in the composition of PSS-*Z*. The procedure was repeated for PSS-*E*, also demonstrating that no spontaneous, thermal *E*-*Z*-isomerization occurs, rendering both polymers bi-stable at 300 K. The thermal stability is of particular importance for the long-term measurements (several hours) in the lyotropic liquid crystalline state, which will be described in the following chapter.

2.3. Photo-Responsive Lyotropic Liquid Crystalline Behavior

Due to their rod-like helical structure, polyaspartates are known to form lyotropic crystalline phases above a system-specific critical concentration c_{crit} .^[31] Thus, to find out whether this is also the case for the (co-)polyaspartates synthesized herein, concentrated samples were prepared in TCE- d_2 and DCM- d_2 as listed in Table 3. In case of anisotropy, signal splitting of the deuterated solvent is observed in ^2H NMR, known as quadrupolar splitting $\Delta\nu_Q$.^[69] For the investigation of the macroscopic change in the LLC phase upon photo-switching, anisotropic samples were

Table 3. LLC phases of (co-)polyaspartates with their respective batch numbers in deuterated solvents with their critical concentration c_{crit} determined by dilution and quadrupolar splitting at PSS-Z and PSS-E at concentration c_{set} . No LLC phase with the homopolymer PmFABLA and the copolymer PpFABLA-Ph₅₀-co-PPLA₅₀ could be prepared. We assume this to be due to low molecular weight of the obtained polymer of PmFABLA and due to insufficient solubility of the PpFABLA-Ph₅₀-co-PPLA₅₀. Polymers with photo-responsive helix-to-helix transition (helix inversion) in diluted solutions and a change of quadrupolar splitting in magnitude and sign in LLC phase are highlighted in orange.

Entry	Polymer	Solvent	$c_{\text{crit}}^{\text{b)}}$ /wt.%	c_{set} /wt.%	$\Delta v_{\text{Q,PSS-Z}}$ /Hz	$\Delta v_{\text{Q,PSS-E}}$ /Hz	RH-LLC-##	Batch
1	PpFABLA ₇₅ -co-PBLA ₂₅	TCE- <i>d</i> ₂	15.0	18.2	339	335	08	204
2	PpFABLA ₅₀ -co-PBLA ₅₀	TCE- <i>d</i> ₂	12.5	14.1	238	330	09	201
3	PpFABLA ₂₅ -co-PBLA ₇₅	TCE- <i>d</i> ₂	10.5	13.9	369	383	21	206
4	PpFABLA ₇₅ -co-PPLA ₂₅	TCE- <i>d</i> ₂	15.0	17.6	223	219	06	205
5	PpFABLA ₅₀ -co-PPLA ₅₀	TCE- <i>d</i> ₂	15.0	19.9	-41	270	17	202
6	PpFABLA ₂₅ -co-PPLA ₇₅	TCE- <i>d</i> ₂	11.0	11.6	-207	-165	35	207
7	PmFABLA ₇₅ -co-PBLA ₂₅	TCE- <i>d</i> ₂	19.5	22.1	61	-189	14_2	261
8	PmFABLA ₅₀ -co-PBLA ₅₀	TCE- <i>d</i> ₂	16.5	17.0	241	366	15	262
9	PmFABLA ₂₅ -co-PBLA ₇₅	TCE- <i>d</i> ₂	13.0	15.0	253	343	16	263
10	PmFABLA ₇₅ -co-PPLA ₂₅	TCE- <i>d</i> ₂	18.5	19.1	-190	-29	11	258
11	PmFABLA ₅₀ -co-PPLA ₅₀	TCE- <i>d</i> ₂	14.0	15.2	-236	52	12	259
12	PmFABLA ₂₅ -co-PPLA ₇₅	TCE- <i>d</i> ₂	10.5	12.4	-290	-241	13	260
13	PpFABLA	TCE- <i>d</i> ₂	21.0	23.6	0	282	65	301
14	PpFABLA-C6	TCE- <i>d</i> ₂	14.0	15.7	109	52	26	275
15 ^{a)}	PpFABLA-C12	TCE- <i>d</i> ₂	n.d.	28.7	≈240	325	30	295
16	PpFABLA-C6 ₅₀ -co-PPLA ₅₀	TCE- <i>d</i> ₂	17.0	24.5	-216	315	27	293
17	PpFABLA-C12 ₅₀ -co-PPLA ₅₀	TCE- <i>d</i> ₂	23.0	26.7	-33	372	28	294
18	PpFABLA	DCM- <i>d</i> ₂	23.0	26.2	85	137	48	301
19	PpFABLA-C6	DCM- <i>d</i> ₂	33.0	36.6	180	>430	43	NS02-14
20	PpFABLA-C12	DCM- <i>d</i> ₂	n.d.	25.0	137	>430	49_3	NS02-13
21	PpFABLA-co-PPLA	DCM- <i>d</i> ₂	15.5	16.9	34	94	42	300
22	PpFABLA-C6 ₅₀ -co-PPLA ₅₀	DCM- <i>d</i> ₂	21.5	22.8	55	217	52	293
23	PpFABLA-C12 ₅₀ -co-PPLA ₅₀	DCM- <i>d</i> ₂	20.5	31.9	97	293	54	294

n.d. = not determined. ^{a)} For PpFABLA-C12 in TCE-*d*₂ (entry 15), only a partially anisotropic sample could be prepared irrespective of the sample concentration and photo-isomerization. It is presumed, that the low molecular weight of the polymer does not allow for the formation of a stable LLC-phase in PSS-E. Photo-isomerization from E→Z leads to an increase of the isotropic signal at the same sample concentration. The quadrupolar splitting is determined from the partially anisotropic state of the LLC phase for the estimation of the change of quadrupolar splitting upon photoisomerization. Due to insufficient spectral quality, the sign of quadrupolar splitting was assumed to be positive and not determined via Q.E.COSY spectra; ^{b)} Critical concentrations are given with an estimated uncertainty of ± 0.5 wt.%.

irradiated ex situ at 405 and 520 nm to interconvert E- and Z-isomers, respectively. The irradiation series is monitored by ²H NMR spectroscopy by determining the magnitude of quadrupolar splitting after each irradiation step (see SI for a more detailed depiction of ²H NMR series). Photo-stationary states were determined as the point at which no further change in quadrupolar splitting was observed upon additional irradiation. The signs of quadrupolar splittings were obtained from Q.E.COSY experiments.^[70] The quantification of isomeric ratios in anisotropic samples via ¹⁹F NMR-spectroscopy was not possible due to significant signal broadening and overlap (see SI).

A comparison of the quadrupolar splitting in PSS-Z and PSS-E shows the photo-response within one LLC phase. From a first glance at Table 3, it is noticed that polymers with a significant change in backbone conformation also show a significant photo-responsive behavior in the LLC phase with large changes in the size of quadrupolar splitting and changes of the sign. The photo-responsive LLC behavior of polymers without significant photo-induced conformational changes in TCE-*d*₂ is only accompanied by small changes in quadrupolar splitting as depicted exemplarily for the PpFABLA₇₅-co-PPLA₂₅ in TCE-*d*₂

(Table 3, entry 4) in Figure 4a (for a detailed depiction of ²H NMR series for all obtained polymers, see SI). The irradiation series was started by ex situ irradiation with green light ($\lambda = 520$ nm) inducing isomerization from E- to Z-species until a stationary state was reached, where a quadrupolar splitting of -208 Hz was obtained in PSS-Z. The PSS-E was produced by irradiation at 405 nm resulting in a quadrupolar splitting of -165 Hz. This change only in size but not sign implies that no significant reorientation of the LLC order experienced by the solvent is induced by switching between the two photo-stationary states. It is assumed that the side chain conformation has an influence on the rigidity of the helix and thus impacts the order of the liquid crystalline phase, but that no significant reorientation within the LLC phase is present. Further investigations regarding the photo-responsive reorientation of the mesogens could be carried out if deuterated analogs of the polymers were obtained and studied for their LLC behavior. Then, the quadrupolar splitting resulting from the deuterated polymer could be investigated, which would give direct information about the orientation of the mesogens. This could be correlated with the quadrupolar splitting of the solvent as shown in our previous work.^[33,71]

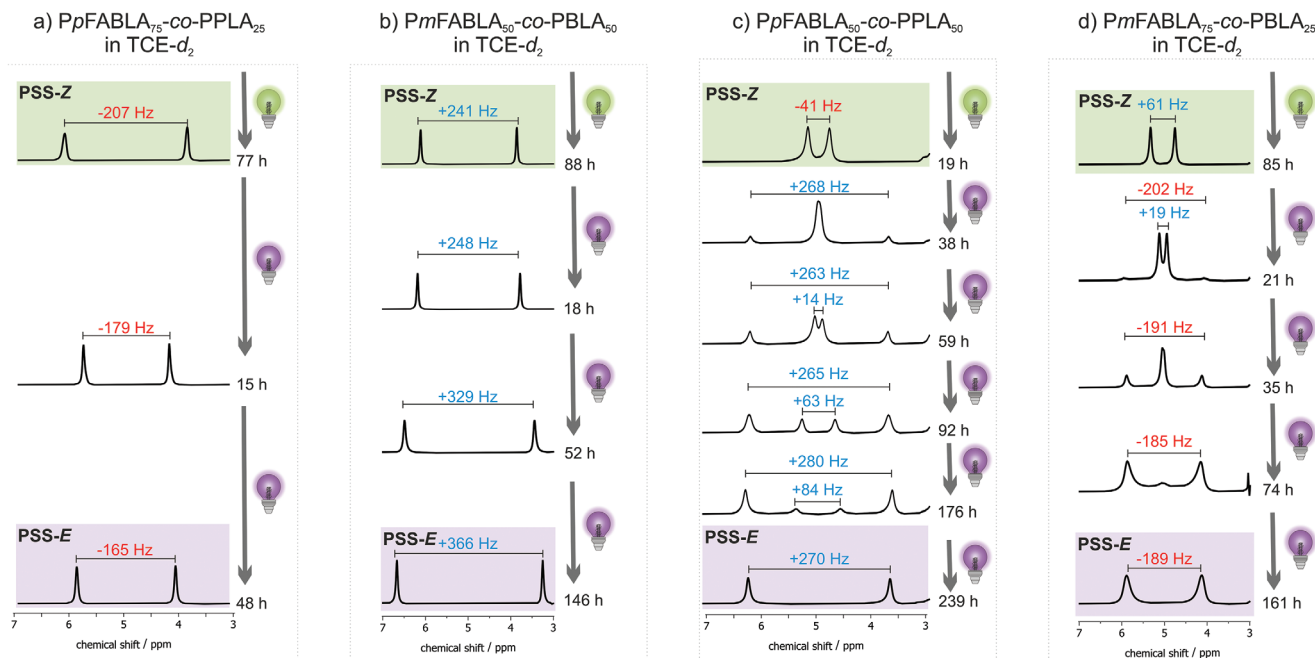


Figure 4. Series of ^2H NMR spectra (107 MHz, 300 K) of LLC phases in $\text{TCE-}d_2$ upon ex situ irradiation at 520 nm ($E \rightarrow Z$) and 405 nm ($Z \rightarrow E$): a) LLC-06 with $\text{PpFABLA}_{75}\text{-co-PPLA}_{25}$, b) LLC-15 with $\text{PmFABLA}_{50}\text{-co-PBLA}_{50}$, c) LLC-17 with $\text{PpFABLA}_{50}\text{-co-PPLA}_{50}$ and d) LLC-14_2 with $\text{PmFABLA}_{75}\text{-co-PBLA}_{25}$.

In general, polymers with non-switchable helicity show a similar behavior in the LLC phase, where decreasing helicity in isotropic solution correlates with decreasing quadrupolar splitting in LLC phase, indicating a less ordered liquid crystalline environment (see Table 3, entries 1–3, 6, 9, 10, 12, 14). For the LLC phase of $\text{PmFABLA}_{50}\text{-co-PBLA}_{50}$ in $\text{TCE-}d_2$ (Figure 4b, Table 3, entry 8), the preservation of anisotropy is observed in every measured state. These findings support the interpretation that the previously discussed $\text{CD} = 0$ cases in PSS-Z (e.g., Table 2, entry 11) occur due to equal amounts of α_L and α_R helix and not due to a random coil structure being present.

Compared to these LLC phases based on stable helices, the liquid crystalline behavior of helix inversion polymers $\text{PpFABLA}_{50}\text{-co-PPLA}_{50}$ (Figure 4c, Table 3, entry 5) and $\text{PmFABLA}_{75}\text{-co-PBLA}_{25}$ (Figure 4d, Table 3, entry 7) upon irradiation is more complex. The LLC phase consisting of $\text{PpFABLA}_{50}\text{-co-PPLA}_{50}$ in $\text{TCE-}d_2$ (Table 3, entry 5) exhibits a quadrupolar splitting of -41 Hz in PSS-Z. Subsequently, the $Z \rightarrow E$ transition is induced with violet light producing higher contents of the E -species in the concentrated sample with every irradiation step. Interim states between both PSS show the evolution of two distinct sets of signals in the ^2H NMR spectra, which are interpreted as different liquid crystalline domains in the sample being present, which can be rationalized by the different polarity and geometry of E - and Z -isomers. Therefore, E - Z -isomerization in the polymer sidechain forces the phase morphology to change dependent on the isomeric ratio. Ultimately, the PSS- E is reached after irradiation with violet light for 239 h in total giving one signal set with a splitting of $+270$ Hz. The change in sign of the quadrupolar splitting is indicative of a significant reorientation of the solvent in the magnetic field induced by the helix inversion of the polymer chains. The same procedure was applied to an anisotropic sample consisting of $\text{PmFABLA}_{75}\text{-co-PBLA}_{25}$ in TCE-

d_2 (Table 3, entry 7 and Figure 4d) resulting in a similar phase behavior. Here, the quadrupolar splitting also changes in size and sign ($+61$ Hz in PSS-Z and -189 Hz in PSS- E) upon isomerization. Again, the observed change in morphology is proposed to result from a reorientation of the solvent and presumably the mesogen. For the interim states, again two sets of signals are observed, related to the changing LLC order of the domains being present in the sample. With progressive irradiation the quadrupolar splitting of the solvent in domains initially present in PSS-Z decreases until it disappears completely, without going through a sign change as in the case of the $\text{PpFABLA}_{50}\text{-co-PPLA}_{50}$ copolymer discussed above. LLC phases of the other helix inversion polymers $\text{PpFABLA-C6}_{50}\text{-co-PPLA}_{50}$ (Table 3, entry 16) and $\text{PpFABLA-C12}_{50}\text{-co-PPLA}_{50}$ (Table 3, entry 17) in $\text{TCE-}d_2$ show a similar behavior as $\text{PpFABLA}_{50}\text{-co-PPLA}_{50}$. The incorporated alkyl groups lead to LLC phases with lower viscosity despite very high polymer concentrations confirming the solubility-imparting effect.

For the parent homopolymer PpFABLA in PSS- E a stable LLC phase was prepared, but with progressive irradiation at 520 nm polymer precipitation was observed indicating a decreased solubility of the Z -species in TCE (Table 3, entry 13). This leads to a decreased concentration of polymer in solution such that an isotropic signal is observed if the concentration drops below the critical concentration. One possible explanation of this differing result from the literature^[58] could be the lower averaged molecular weight for the PpFABLA homopolymer presented here. In our previous studies, we have shown that the solubility and the ability to form LLC phases depend strongly on the obtained molecular weight. Only polymers in a specific range of molecular weight were able to form LLC phases for PBLA .^[59] It is suggested that a similar behavior could be present for PpFABLA . The improved solubility for homopolymer

PpFABLA-C6 in both PSS is demonstrated such that the liquid crystallinity is preserved (Table 3, entry 14). For the PpFABLA-C12 homopolymer only a partially anisotropic sample could be prepared in TCE- d_2 (Table 3, entry 15), irrespective of the sample concentration or the photo-isomerization. A comparison of the isotropic and anisotropic content in the ^2H NMR of PSS-E ($\approx 43\%$ anisotropic) and PSS-Z ($\approx 20\%$ anisotropic) shows that photo-isomerization from E \rightarrow Z leads to an increase of the isotropic signal. This observation confirms that the helical content decreases with photo-isomerization to the Z-isomer. In general, we observe the quadrupolar splitting of the anisotropic signal to decrease upon photo-isomerization from PSS-E to PSS-Z for the homopolymers with *para*-substituted FAB moieties in the sidechain. We believe this to occur due to a decrease in the helical content of the polymer upon photo-isomerization.

Furthermore, the effect of the solvent on the photo-responsive liquid crystalline behavior was investigated by exchanging TCE- d_2 for DCM- d_2 (see SI). As expected from the chiroptic behavior in DCM, the *para*-substituted copolyaspartates (Table 3, entries 21–23) showed only changes in size, but not in signs of quadrupolar splitting. Interestingly, the homopolymer PpFABLA forms a stable LLC phase in DCM- d_2 (Table 3, entry 18) irrespective of E-Z-isomerization. Only a change in size of the quadrupolar splitting is observed. This supports the interpretation that insufficient solubility of PSS-Z in TCE- d_2 causes the isotropic behavior discussed above. In this context, also PpFABLA-C6 and PpFABLA-C12 exhibit similar behavior in DCM- d_2 (Table 3, entries 19–20).

The LLC-behavior upon photo-switching in DCM- d_2 correlates with the results of CD measurements in DCM as no change of secondary structure is observed. Therefore, only minor changes in the liquid crystalline state were expected. These investigations substantiated, that the photo-responsive secondary structure has a significant influence on the photo-control in the LLC phase impacting the order and morphology with more drastic changes in the liquid crystal being observed for systems with larger changes in secondary structure.

3. Conclusion and Outlook

Novel (co-)polyaspartates with various *ortho*-fluorinated azobenzenes (FABs) in the sidechain were synthesized successfully using an optimized and easily adaptable synthesis route. FAB-moieties possess promising properties as both photo-isomers are thermally stable at ambient temperature and photo-isomerization can be triggered by visible light. The influence of photo-induced E-Z-isomerization of FAB moieties on the conformation of (co-)polymer backbone was investigated in dilute solution via CD spectroscopy. Various reversible transitions (helix-to-random coil and helix inversion) were observed depending on the composition of the polymer. Incorporation of FAB-groups via *para*- and *meta*-substitution has a large impact on the polymer conformation in the photo-stationary states (PSS) for the homopolyaspartates. While *para*-substitution leads to left-handed helices in PSS-E and a decrease in helicity in PSS-Z, *meta*-substitution results in an α_R -helix-to-coil transition upon E-Z-isomerization. The combination of sidechains bearing FAB-groups and non-switchable groups favoring opposing helical senses enabled the reversible interconversion between left- and right-handed helices. Additionally, alkyl groups were introduced,

enhancing solubility in concentrated samples. Thermal stability of the composition of each PSS was demonstrated exemplary for PpFABLA₅₀-co-PPLA₅₀ and PmFABLA₇₅-co-PBLA₂₅ via ^{19}F NMR investigations ensuring reproducible photo-switching behavior. Most (co-)polyaspartates synthesized allowed the preparation of lyotropic liquid crystalline (LLC) phases in TCE- d_2 and DCM- d_2 , which were investigated for their photo-responsivity by NMR spectroscopy. While in TCE different conformational transitions can be observed, stable, non-switchable secondary structures were obtained in DCM as solvent.

Furthermore, from the change in quadrupolar splitting of the deuterated solvent it is deduced, that polymers with large photo-responsive conformational changes (e.g., helix-to-helix) in dilute solution show significant changes in the LLC morphology. This allows the LLC order to be controlled by irradiation with visible light inducing E-Z-isomerization of the FAB moieties in the polymer sidechain. Helix inversion polymers show major photo-responsive behavior in liquid crystalline state and therefore shall be exploited as photo-responsive alignment media for structure elucidation in the future.

Supporting Information

Supporting Information is available from the Wiley Online Library or from the author.

Acknowledgements

R.H. thanks the Avicenna-Studienwerk e.V. for a Ph.D. scholarship. The authors thank Christopher Roß and Lukas Laux for SEC measurements, Jonas Kind and Patrick Maibach for building customized irradiation boxes, Max Hirschmann for scientific discussions, Julia Illic and Nils Sauer for their assistance with polymer synthesis, and Alexander Schießler and the mass spectrometry core facility team for measurements of the ESI and EI/CI spectra and the German Research Foundation (DFG) through grant no INST 163/444-1 FUGG (QTOF) and INST 163/720-1 FUGG (HR EI/CI-GCMS).

Open access funding enabled and organized by Projekt DEAL.

Conflict of Interest

The authors declare no conflict of interest.

Data Availability Statement

The data that support the findings of this study are available from the corresponding author upon reasonable request.

Keywords

azobenzene, helical polymer, liquid crystal, photoswitchable polyaspartates

Received: June 27, 2024

Revised: July 30, 2024

Published online: August 20, 2024

[1] W. B. Spillman, J. S. Sirkis, P. T. Gardiner, *Smart Mater. Struct.* **1996**, *5*, 247.

- [2] S. Bahl, H. Nagar, I. Singh, S. Sehgal, *Mater. Today Proc.* **2020**, *28*, 1302.
- [3] M. Su, Y. Song, *Chem. Rev.* **2022**, *122*, 5144.
- [4] M. Ku, J. C. Hwang, B. Oh, J.-U. Park, *Adv. Intell. Syst.* **2020**, *2*, 1900144.
- [5] Z. Guo, H. Liu, W. Dai, Y. Lei, *Smart Mater. Med.* **2020**, *1*, 54.
- [6] K. I. S. Mabape, C. Donga, S. B. Mishra, A. K. S. Mishra, in *Smart Polymer Catalysts and Tunable Catalysis*, Elsevier, Amsterdam, The Netherlands **2019**, pp. 77–94.
- [7] W. Zhao, Y. Zhao, Q. Wang, T. Liu, J. Sun, R. Zhang, *Small* **2019**, *15*, 1903060.
- [8] M. Aflori, *Nanomaterials* **2021**, *11*, 396.
- [9] D. Yu, X. Xiao, C. Shokoochi, Y. Wang, L. Sun, Z. Juan, M. J. Kipper, J. Tang, L. Huang, G. S. Han, H. S. Jung, J. Chen, *Adv. Funct. Mater.* **2023**, *33*, 2211983.
- [10] S. Uredat, A. Gujare, J. Runge, D. Truzzolillo, J. Oberdisse, T. Hellweg, *Phys. Chem. Chem. Phys.* **2024**, *26*, 2732.
- [11] G. Stoychev, A. Kirillova, L. Ionov, *Adv. Opt. Mater.* **2019**, *7*, 1900067.
- [12] H. Cheng, S. Zhang, E. Bai, X. Cao, J. Wang, J. Qi, J. Liu, J. Zhao, L. Zhang, J. Yoon, *Adv. Mater.* **2022**, *34*, 2108289.
- [13] M. Irie, T. Fukaminato, K. Matsuda, S. Kobatake, *Chem. Rev.* **2014**, *114*, 12174.
- [14] L. Kortekaas, W. R. Browne, *Chem. Soc. Rev.* **2019**, *48*, 3406.
- [15] M. Clerc, S. Sandlass, O. Rifaie-Graham, J. A. Peterson, N. Bruns, J. Read de Alaniz, L. F. Boesel, *Chem. Soc. Rev.* **2023**, *52*, 8245.
- [16] M. Gao, D. Kwaria, Y. Norikane, Y. Yue, *Nat. Sci.* **2023**, *3*, 220020.
- [17] C. Fedele, T.-P. Ruoko, K. Kuntze, M. Virkki, A. Priimagi, *Photochem. Photobiol. Sci.* **2022**, *21*, 1719.
- [18] A. Natansohn, P. Rochon, *Chem. Rev.* **2002**, *102*, 4139.
- [19] M. A. C. Stuart, W. T. S. Huck, J. Genzer, M. Müller, C. Ober, M. Stamm, G. B. Sukhorukov, I. Szleifer, V. V. Tsukruk, M. Urban, F. Winnik, S. Zauscher, I. Luzinov, S. E. S. Minko, *Nat. Mater.* **2010**, *9*, 101.
- [20] M. Lago-Silva, M. Fernández-Míguez, R. Rodríguez, E. Quiñoá, F. Freire, *Chem. Soc. Rev.* **2024**, *53*, 793.
- [21] C. Bonduelle, *Polym. Chem.* **2018**, *9*, 1517.
- [22] M. D. Zotti, F. Formaggio, M. Crisma, C. Peggion, A. Moretto, C. Toniolo, *J. Pept. Sci.* **2014**, *20*, 307.
- [23] J. F. Yan, G. Vanderkooi, H. A. Scheraga, *J. Chem. Phys.* **1968**, *49*, 2713.
- [24] E. M. Bradbury, B. G. Carpenter, H. Goldman, *Biopolymers* **1968**, *6*, 837.
- [25] M. Goodman, F. Boardman, I. Listowsky, *J. Am. Chem. Soc.* **1963**, *85*, 2491.
- [26] M. Loucheux-Lefebvre, C. Duflo, G. Weill, *Biopolymers* **1975**, *14*, 469.
- [27] M. Hashimoto, *Bull. Chem. Soc. Jpn.* **1966**, *39*, 2713.
- [28] C. Toniolo, E. Benedetti, *Crit. Rev. Biochem.* **1980**, *9*, 1.
- [29] E. R. Blout, R. H. Karlson, *J. Am. Chem. Soc.* **1958**, *80*, 1259.
- [30] A. Ushiyama, H. Furuya, A. Abe, T. Yamazaki, *Polymer J.* **2002**, *34*, 450.
- [31] A. Abe, H. Furuya, S. Okamoto, *Pept. Sci.* **1997**, *43*, 405.
- [32] Y. Imada, A. Abe, *Polymer* **2010**, *51*, 6227.
- [33] M. Hirschmann, D. S. Schirra, C. M. C. Thiele, *Macromolecules* **2021**, *54*, 1648.
- [34] F. Ciardelli, S. Bronco, O. Pieroni, A. Pucci, in *Molecular Switches*, (Eds: B. L. Feringa, W. R. Browne), Wiley, xx xx **2011**, pp. 321–360.
- [35] A. Ueno, J. Anzai, T. Osa, Y. Kadoma, *Bull. Chem. Soc. Jpn.* **1979**, *52*, 549.
- [36] A. Ueno, K. Takahashi, J. Anzai, T. Osa, *Macromolecules* **1980**, *13*, 459.
- [37] A. Ueno, K. Takahashi, J. Anzai, T. Osa, *Bull. Chem. Soc. Jpn.* **1980**, *53*, 1988.
- [38] A. Ueno, K. Adachi, J. Nakamura, T. Osa, *J. Polym. Sci., Part A: Polym. Chem.* **1990**, *28*, 1161.
- [39] D. Bléger, J. Schwarz, A. M. Brouwer, S. Hecht, *J. Am. Chem. Soc.* **2012**, *134*, 20597.
- [40] C. Knie, M. Utecht, F. Zhao, H. Kulla, S. Kovalenko, A. M. Brouwer, P. Saalfrank, S. Hecht, D. Bléger, *Chem. – Eur. J.* **2014**, *20*, 16492.
- [41] N. Tjandra, A. Bax, *Science* **1997**, *278*, 1111.
- [42] C. M. Thiele, *Eur. J. Org. Chem.* **2008**, *2008*, 5673.
- [43] J. Rettig, M. Brauser, C. M. Thiele, in *Residual Dipolar Couplings: Principles and Applications* (Eds: L. Yao, B. Vogeli), Royal Society of Chemistry, Burlington House, Piccadilly, London **2024**, pp. 252–279.
- [44] S. Immel, M. Köck, M. Reggelin, *Chem. – Eur. J.* **2018**, *24*, 13918.
- [45] F. A. Roth, V. Schmidts, J. Rettig, C. M. Thiele, *Phys. Chem. Chem. Phys.* **2022**, *24*, 281.
- [46] J. R. Tolman, *J. Am. Chem. Soc.* **2002**, *124*, 12020.
- [47] W. A. R. Van Heeswijk, M. J. D. Eenink, J. Feijen, *Synthesis* **2002**, *1982*, 744.
- [48] A. Rasines Mazo, S. Allison-Logan, F. Karimi, N. J.-A. Chan, W. Qiu, W. Duan, N. M. O'Brien-Simpson, G. G. Qiao, *Chem. Soc. Rev.* **2020**, *49*, 4737.
- [49] J. Cheng, T. J. Deming, in *Peptide-Based Materials, Topics in Current Chemistry*, Vol. 310, Springer, Berlin, Heidelberg **2011**, pp. 1–26.
- [50] P. Pfaff, K. T. G. Samarasinghe, C. M. Crews, E. M. Carreira, *ACS Cent. Sci.* **2019**, *5*, 1682.
- [51] M. J. Hansen, M. M. Lerch, W. Szymanski, B. L. Feringa, *Angew. Chem., Int. Ed.* **2016**, *55*, 13514.
- [52] J. Gonda, S. Fazekašová, M. Martinková, T. Mitříková, D. Roman, M. B. Pilátová, *Org. Biomol. Chem.* **2019**, *17*, 3361.
- [53] N. M. B. Smeets, P. L. J. van der Weide, J. Meuldijk, J. A. J. M. Vekemans, L. A. Hulshof, *Org. Process Res. Dev.* **2005**, *9*, 757.
- [54] M. Schwab, D. Herold, C. M. Thiele, *Chem. – Eur. J.* **2017**, *23*, 14576.
- [55] W. D. Fuller, M. S. Verlander, M. Goodman, *Biopolymers* **1976**, *15*, 1869.
- [56] R. Albert, J. Danklmaier, H. Hönig, H. Kandolf, *Synthesis* **1987**, *1987*, 635.
- [57] W. Zhao, Y. Gnanou, N. Hadjichristidis, *Polym. Chem.* **2015**, *6*, 6193.
- [58] M. Hirschmann, O. Soltwedel, P. Ritzert, R. von Klitzing, C. M. Thiele, *J. Am. Chem. Soc.* **2023**, *145*, 3615.
- [59] M. Hirschmann, M. Schwab, C. M. Thiele, *Macromolecules* **2019**, *52*, 6025.
- [60] T. Hashimoto, T. Ijitsu, K. Yamaguchi, H. Kawai, *Polymer J.* **1980**, *12*, 745.
- [61] J. M. Montserrat, S. Muñoz-Guerra, J. A. Subirana, *Makromol. Chem. Macromol. Symp.* **1988**, *20–21*, 319.
- [62] B. M. Bulheller, A. Rodger, J. D. Hirst, *Phys. Chem. Chem. Phys.* **2007**, *9*, 2020.
- [63] M. Hirschmann, C. Merten, C. M. Thiele, *Soft Matter* **2021**, *17*, 2849.
- [64] P. Doty, J. H. Bradbury, A. M. Holtzer, *J. Am. Chem. Soc.* **1956**, *78*, 8.
- [65] A. Rodger, in *Encyclopedia of Biophysics* (Ed: G. C. K. Roberts), Springer, Berlin, Heidelberg **2013**, pp. 311–313.
- [66] M. J. Kim, S. J. Yoo, D. Y. Kim, *Adv. Funct. Mater.* **2006**, *16*, 2089.
- [67] G. Pescitelli, *Chirality* **2022**, *34*, 333.
- [68] E. M. Bradbury, L. Brown, A. R. Downie, A. Elliott, W. E. Hanby, T. R. R. McDonald, *Nature* **1959**, *183*, 1736.
- [69] A. S. Ulrich, S. L. Grage, in *Studies in Physical and Theoretical Chemistry*, Vol. 84, Elsevier, **1998**, pp. 190–211.
- [70] P. Zvetkova, B. Q. E. Luy, *Magn. Reson. Chem.* **2016**, *54*, 351.
- [71] D. S. Schirra, M. Hirschmann, I. A. Radulov, M. Lehmann, C. M. Thiele, *Angew. Chem.* **2021**, *133*, 21208.
- [72] These findings differ from those reported previously in literature[58] for the PpFABLA homopolymer, where a helix-coil transition or complete collapse of the helical structure upon photo-isomerization from E→Z is observed. One potential explanation for this slightly different behavior could be the difference in molecular weight, which can have a major impact on the formation and resulting stability of the helix.

Especially, for polyaspartates in the range of low molecular weights a dependency of the helix stability is reported. In these cases, the secondary structure is particularly sensitive to changes in temperature and solvent composition [64].

[73] After irradiation of PmFABLA75-co-PBLA75 in the irradiation box the equilibrium in the NMR at 300 K is reached after ≈ 5 h. A minor

change in the composition of the PSSs at the beginning of monitoring is observed. We believe this to be due to the temperature of the polymer solution during irradiation in the customized boxes probably deviating from 300 K, as irradiation for a long time leads to heating of the sample. For the irradiation box with 520 nm, the box temperature is regulated to 23 °C.